

# Physics-Based Characterization of UXO from Multi-Component TEM Data

Scott C. MacInnes, Donald D. Snyder, and Kenneth L. Zonge  
Zonge Engineering & Research Organization  
3322 E Fort Lowell Rd  
Tucson, AZ, 85716  
(520) 327-5501; FAX (520) 325-1588  
[zonge@alaska.net](mailto:zonge@alaska.net)

Detection, Including Discrimination

## Abstract

Newly developed transient electromagnetic (TEM) equipment collects four-dimensional data with three dB/dt components and time variation. Transient data from three receiver loops are recorded at 31 delay times, ranging from 1 to 1900  $\mu$ sec, and transients are recorded 32 times per second, generating high-density data sets. The equipment is flexible, transmitter and receiver loops can be reconfigured to optimize survey results based on expected target characteristics. With such large data sets and variable equipment configuration, modeling plays an important role. Inversion to dipolar models extracts physically meaningful target parameters from high-density TEM data.

Patches of TEM data near target anomalies are parameterized with the widely used anisotropic dipole model [1]. Three orthogonal magnetic dipoles are used to represent target polarizability along three axes. Spatial variation of receiver loop dB/dt across the data patch is projected onto three, generally tilted target axes, compressing data from hundreds of measurement positions and multiple loop orientations into three polarizability values for each transient delay time. Time-dependent target properties are parameterized by fitting a transient-shape model to the polarizability transient for each of the three target axes.

Targets can be characterized by these physics-based model parameters [2]–[4]. Transient shape is influenced by target size, shape, conductivity and permeability. Polarizability magnitude is proportional to target volume. Ratios of target-axis polarizability are indicative of target symmetry. We present application of our modeling routines to multi-component data obtained from a demonstration survey at NRL UXO test site located at the Army Research Lab facility at Blossom Point, MD.

## Introduction

When mapping an area to locate UXO it is convenient to use a portable TEM system with a horizontal transmitter loop and three receiver loops arranged to measure multiple magnetic field components (Figure 1). A cart-mounted Dynamic NanoTEM (DNT) system with a 1 by 1 m horizontal loop transmitter and three orthogonal 0.5 by 0.5 m receiver loops was used for data acquisition at the Blossom Point Test Range.

The same loop configuration can be placed on the ground for more careful follow-up measurements. Static follow up measurements are generally averaged over a large number of transmitter waveform cycles to suppress background noise, and putting the loops directly on the ground significantly increases signal strength by reducing the separation between loops and target.



**Figure 1: Mapping with a cart-mounted Dynamic NanoTEM (DNT) system.**

Electromagnetic source fields are generated by driving square current pulses of alternating polarity separated by zero current measurement intervals through the transmitter loop (Figure 2). When the transmitter current is switched off, the abrupt collapse of the transmitter loop's magnetic field produces strong dB/dt pulse. Weak secondary dB/dt from conductive subsurface objects can be detected with receiver loops during the intervals between current pulses. Orthogonal receiver loops measure both the secondary field magnitude and its orientation.

Time-varying properties of the target's response are of interest, so transient values are recorded at 31 logarithmically spaced times ranging from 0.5 to 2000  $\mu\text{sec}$ . Transients are affected by an object's shape, size, conductivity and permeability.

Induced currents decay more slowly in larger, more conductive or more permeable objects. A target's shape affects its response; rod-like ferrous objects have a more persistent signal along their longitudinal axis than along their shorter transverse axes. Ferrous disks have a less persistent response along their short longitudinal axis than along their two transverse axes. The relationship is reversed for non-ferrous objects. An aluminum disk has a more persistent response along its longitudinal axis. Objects with cylindrical symmetry have the same response on their two transverse axes, while irregular shapes are likely to have a different response to source-field illumination along each axis.

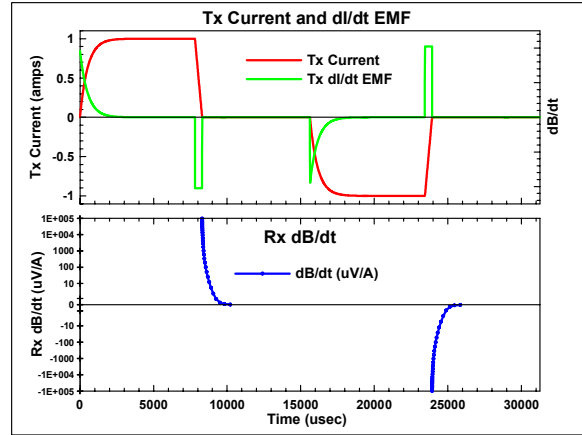


**Figure 2: Transmitter current and receiver dB/dt waveforms.**

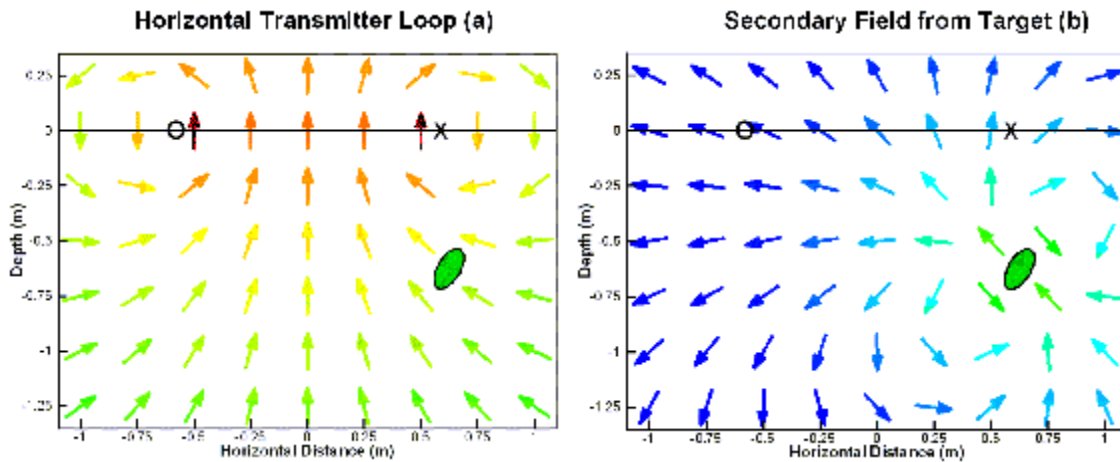


**Figure 3: Magnetic field vector direction and amplitude.**

The magnetic field is nearly vertical directly under a horizontal transmitter loop (Figure 3a). As the transmitter loop is displaced sideways from a UXO, its field becomes more tilted. To thoroughly test the electrical behavior of a conductive object, it must be illuminated by the transmitter loop's magnetic field from enough different directions to excite responses along all three target axes. Induced currents in a conductive target produce dipolar secondary fields (Figure 3b), which are "interrogated" by receiver loops. The induced dipole may have a different orientation than the illuminating source field due to effects of target shape, so receiver loop orientations and positions must be varied enough to map both the position and orientation of induced target dipoles.

## Dipole Model

An anisotropic dipole model is suitable for predicting the response of compact, conductive objects in a resistive background. Inductive coupling between transmitter loop and target is represented by  $\bar{H}_{Tx}(\bar{r}')$ , the free-space magnetic field at the target generated by a unit current in the transmitter loop. As the transmitter current pulse is shut off it illuminates the target with a  $d\bar{B}/dt$  spike, inducing a dipolar polarization,  $\bar{M}(t, \bar{r}') = \bar{P}(t) \cdot \bar{H}_{Tx}(\bar{r}') \cdot \delta(t)$ . The target's polarization,  $\bar{M}(t, \bar{r}')$ , typically has a different orientation than the transmitter's magnetic field due to the target's elongation and tilt. Inductive coupling between the polarized target and each receiver loop is represented by  $\bar{H}_{Rx}(\bar{r})$ .

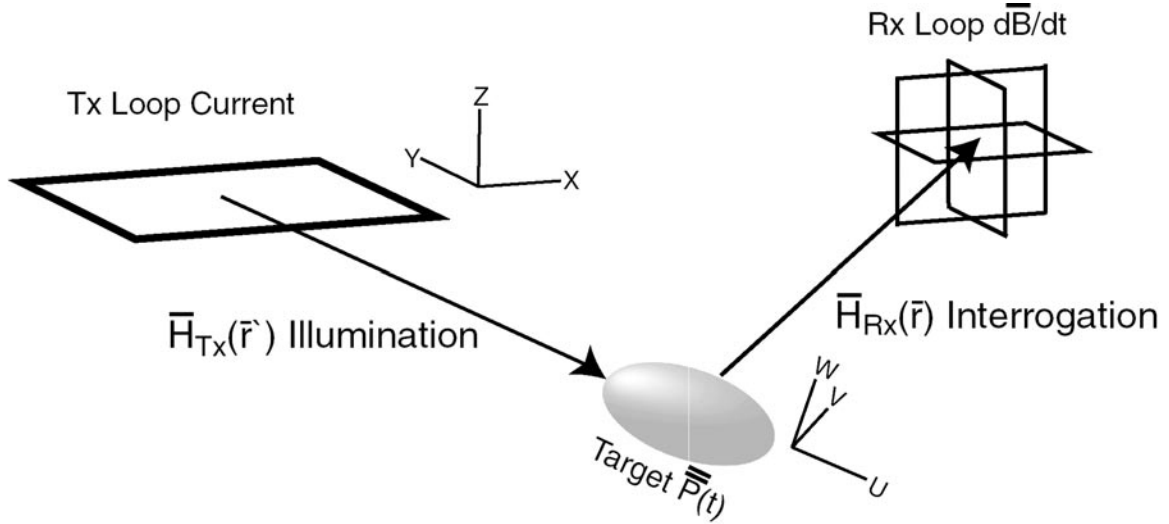


Figure 4: Schematic of anisotropic dipole model.

The inductive link from transmitter loop current to target polarization and back to a receiver loop  $d\bar{B}/dt$  can be represented by

$$\frac{d\bar{B}(\bar{r}, t, \bar{r}')}{dt} = \mu_0 \cdot \bar{H}_{Rx}(\bar{r}) \cdot \bar{P}(t) \cdot \bar{H}_{Tx}(\bar{r}') \cdot \delta(t)$$

$\bar{H}_{Tx}(\bar{r}')$  and  $\bar{H}_{Rx}(\bar{r})$  are dependent upon the locations of transmitter and receiver loops relative to the target. The model's dependence upon target  $(x, y, z)$  is contained in  $\bar{H}_{Tx}(\bar{r}')$  and  $\bar{H}_{Rx}(\bar{r})$  which each have units of  $1/m^3$ . All of the target's time-dependant behavior is described by the tensor polarizability,  $\bar{P}(t)$ .

For TEM modeling, convenient units for  $\bar{P}(t)$  are  $cm^3/\mu sec = m^3/sec$ .

$$\bar{P}(t) = \begin{bmatrix} p_{xx}(t) & p_{xy}(t) & p_{xz}(t) \\ p_{yx}(t) & p_{yy}(t) & p_{yz}(t) \\ p_{zx}(t) & p_{zy}(t) & p_{zz}(t) \end{bmatrix} = \overline{\overline{R(\theta, \phi, \varphi)}}^t \cdot \begin{bmatrix} p_u(t) & 0 & 0 \\ 0 & p_v(t) & 0 \\ 0 & 0 & p_w(t) \end{bmatrix} \cdot \overline{\overline{R(\theta, \phi, \varphi)}}$$

$\bar{P}(t)$  is a symmetric polarizability tensor which can be diagonalized by a rotation from geographic  $(x, y, z)$  to target axes  $(u, v, w)$  coordinates. An unrotated polarizability tensor can be parameterized by six parameters  $(p_{xx}, p_{yx} = p_{xy}, p_{yy}, p_{zx} = p_{xz}, p_{zy} = p_{yz}, p_{zz})$ . When rotated, polarizability is a function of  $(\theta, \phi, \varphi, p_u, p_v, p_w)$  where  $\theta, \phi$ , and  $\varphi$  are Euler rotation angles and  $p_u, p_v$ , and  $p_w$  are polarizability values along target axes.

TEM dB/dt transient data can be inverted to recover target properties by rearranging the dipole model to express dB/dt as a function of target (x,y,z) and polarizability. Since all of the target's time-dependant properties are contained in the polarizability tensor, an inversion to recover target position and orientation can be separated from inversion to recover a description of target polarizability time variance.

As Bell, et al [2] point out, given a target (x,y,z) location, inverting  $\overline{d_{obs}}$  to find the elements of an unrotated polarizability tensor is a linear least squares problem. A global inversion method like simulated annealing can be used to select trial values of the non-linear parameters target (x,y,z). For each trial (x,y,z), linear least-squares can be used to solve for the polarizability tensor. The location of the target anomaly peak is a good estimate of target (x,y) and anomaly width is a good estimate of target depth so a nonlinear inversion for target (x,y,z) can be initialized with a good starting model.

Once a satisfactory target location (x,y,z) is established, a singular value decomposition of  $\overline{P(t)}$  yields the coordinate rotation necessary to diagonalize the polarizability tensor. With a target rotation and orientation in hand, the dipole model can be used to project receiver dB/dt onto target axes polarizability. The projection generates observed polarizability data ( $\rho_u(t), \rho_v(t), \rho_w(t)$ ), which compactly describe the target's time dependent behavior. Polarizability for each axis can be parameterized by numerically integrating  $\rho_*(t_i)$  (in  $cm^3/\mu sec$ ) to get a  $\rho_0$  (in  $cm^3$ ) or by using a model like Pasion and Oldenburg's [4]  $\rho(t) = k \cdot \exp(-t/\tau) \cdot (a+t)^{-b}$  to describe time variation.

## Blossom Point Test Data

When traversing a grid area to map UXO, measurements are taken along closely spaced lines, typically separated by one transmitter loop width or less (Figure 5). Saving transients 32 times per second produces data values every 3 cm along line at a typical walking speed of 1 m/sec. Such high data density along line provides plenty of material for low-pass or non-linear filtering to improve signal to noise. As the line may pass to one side of a target object, the cross-line horizontal component is helpful in estimating the target's lateral position relative to the line.

Improved information about UXO properties can be deduced by collecting additional follow-up data. In follow up, static measurements with longer stacking times can reduce dB/dt transient noise levels by a factor of 10 or more. Additionally, loop position and orientation relative to a central survey point can be carefully measured, reducing the uncertainties in loop position and orientation which can degrade data collected with a moving TEM system [2]. Three-component follow-up data were collected at Blossom point over selected anomalies. Figure 6 shows a composite of follow-up transients measured over Blossom Point Target B14. An array with a horizontal transmitter loop and three orthogonal receiver loops was placed on the ground for each measurement. Measurements were made on a 3 by 3 grid with positions offset +/-0.5 m from anomaly center.

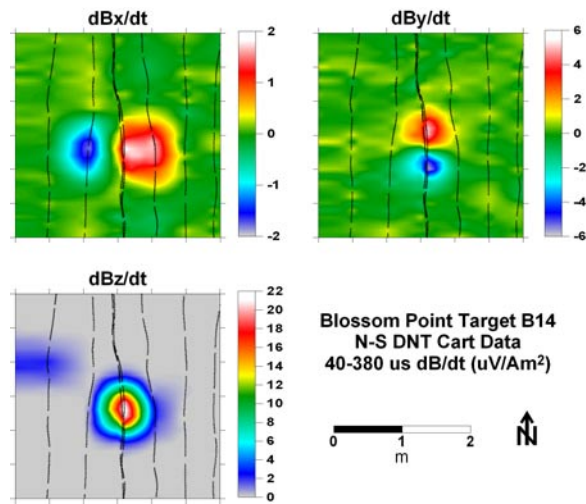


**Figure 5: Plan map images of DNT Cart data at Blossom Point Target B14.**

Inversion DNT data near Blossom Point Target B14 collapses more than 2000 dB/dt transients onto three dP/dt polarizability transients along each of the target object's axes. The target's time-varying response is parameterized by fitting each polarizability transient with a Pasion model. The result for anomaly B14 is consistent with a MK 23, an elongated ferrous object with cylindrical symmetry. Polarization transients for the target's v and w axes are almost the same, while the dPu/dt transient along the targets longitudinal axes

has much greater amplitude. Inversion of 9-spot follow up data for anomaly B14, produces similar model parameters with lower error estimates.

## Summary

Mapping surveys with broadband multi-component TEM generate high density data sets. Follow-up surveys using static measurements provide complimentary data with lower noise levels and more accurate measurement positions. Inversions to anisotropic dipole models extract estimates of UXO location, orientation and time-dependent polarizability properties.

Dipole model parameters provide physics-based criteria for UXO characterization. Once a target position and orientation have been estimated, linear inversion compresses thousands of receiver loop dB/dt values onto three target-axes polarizability transients. Polarizability transient shape is influenced by target size, shape, conductivity and permeability. The vector amplitude of target polarizability is proportional to target volume. Ratios of target-axis polarizability are controlled by target shape and permeability. Anisotropic dipole modeling compresses high-volume data from multi-component modeling to compact sets of model parameters that are closely tied to physical target properties.

## Acknowledgement

This work is supported by the Environmental Security Technology Certification Program (ESTCP) under contract No. DACA72-01-C-0029, "UXO Characterization with a Fast 4-D TEM System".

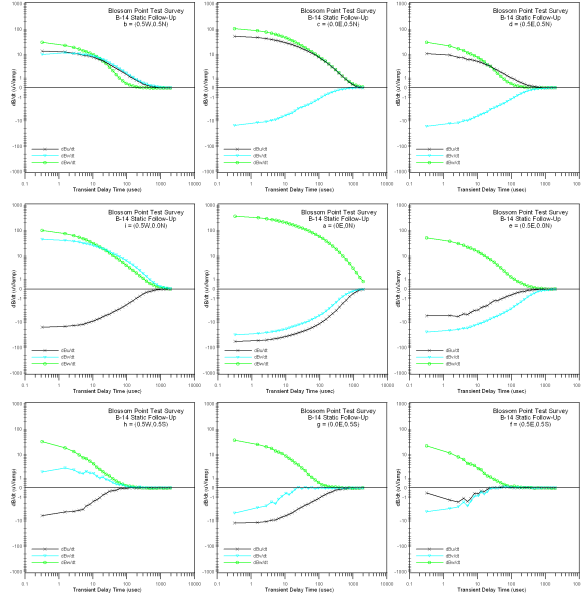


Figure 6: Blossom Point B14, 9-spot transients

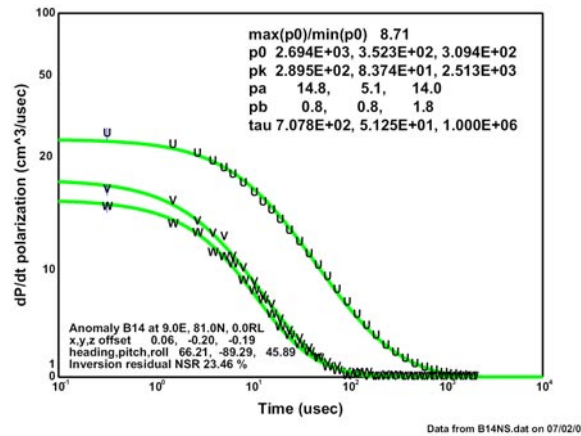


Figure 7: Target B14 polarizability transients from inversion of north-south cart data.

## References

- [1] Das, Y., McFee, J.E., Toews, J., Stuart, G.C., 1990, Analysis of an electromagnetic induction detector for real-time location of buried object, IEEE Tran. on Geos. and Remote Sensing, v28, pp278-288.
- [2] Barrow, B. and Nelson, H.H., 2001, Model-based characterization of electromagnetic induction signatures obtained with the MTADS electromagnetic array, IEEE Tran. on Geos. and Remote Sensing, v39, pp1279-1285.
- [3] Bell, T.H., Barrow, J., Miller, J.T., 2001, Subsurface discrimination using electromagnetic induction sensors, IEEE Tran. on Geos. and Remote Sensing, v39, pp1286-1293.
- [4] Pasion, L.R., Oldenburg, D.W., 1999, Locating and determining dimensionality of UXOs using time domain induction, in SAGEEP 1999, Oakland, CA.